HHS Public Access

Author manuscript

Arterioscler Thromb Vasc Biol. Author manuscript; available in PMC 2020 September 01.

Published in final edited form as:

Arterioscler Thromb Vasc Biol. 2019 September ; 39(9): 1817–1830. doi:10.1161/ATVBAHA.119.312848.

Formation and Resolution of Pial Microvascular Thrombosis in a Mouse Model of Thrombotic Thrombocytopenic Purpura

Reheman Adili[1,*], **Michael Holinstat**[1,2,*]

[1]Department of Pharmacology, University of Michigan, Ann Arbor, MI

[2]Department of Internal Medicine, Division of Cardiovascular Medicine, University of Michigan, Ann Arbor, MI

Abstract

Objective: Microvascular thrombosis is the hallmark pathology of thrombotic thrombocytopenic purpura (TTP), a rare life-threatening disease. Neurologic dysfunction is present in over 90% of TTP patients, and TTP can cause long-lasting neurological damage or death. However, the pathophysiology of microvascular thrombosis in the brain is not well-studied to date. Here, we investigate the formation, and resolution of thrombosis in pial microvessels.

Approach and Results: Using a cranial intravital microscopy in well-established mouse models of congenital TTP induced by infusion of recombinant von Willebrand factor (VWF), we found that soluble VWF, at high concentration, adheres to the endothelium of the vessel wall, self-associates, and initiates platelet adhesion resulting in the formation of pial microvascular thrombosis in ADAMTS13$^{-/-}$ mice. Importantly, VWF-mediated pial microvascular thrombosis occurred without vascular injury to the brain and thrombi consisted of resting platelets adhered onto ultra large VWF without fibrin in the brain in rVWF challenged ADAMTS13$^{-/-}$ mice. Prophylactic treatment with recombinant ADAMTS13 (BAX930) effectively prevented the onset of the VWF-mediated microvascular thrombosis and therapeutic treatment with BAX930 acutely resolved the preexisting or growing thrombi in the brain of ADAMTS13$^{-/-}$ mice following rVWF challenge. The absence of platelet activation and fibrin formation within VWF-mediated thrombi and efficacy of BAX930 was confirmed with an endothelial-driven VWF-mediated microvascular thrombosis model in mice.

Conclusions: Our results provide important insight into the initiation and development of microvascular thrombi in mouse models that mimics TTP and indicate that rADAMTS13 could be an effective interventional therapy for microvascular thrombosis, the hallmark pathology in TTP.

Corresponding authors **Address correspondence to:** Reheman Adili, M.D, Department of Pharmacology, University of Michigan Medical School, 1150 W. Medical Center Dr., Room 2240, Medical Sciences Research Building III, Ann Arbor, MI 48109-5632. Phone: 734-763-8824; Fax: 734-763-4450; rehemana@med.umich.edu; Or, Michael Holinstat, Ph.D., Department of Pharmacology, University of Michigan Medical School, 1150 W. Medical Center Dr., Room 2220D, Medical Sciences Research Building III, Ann Arbor, MI 48109-5632, Phone: 734-764-4046; Fax: 734-763-4450; mholinst@umich.edu.

*These authors contributed equally to this article.

Disclosure of conflict of interest

Drs. Holinstat and Adili received financial support from Shire for the research presented here. Dr. Holinstat is a consultant and equity holder for Veralox Therapeutics, although no work presented here is associated with the relationship with Veralox Therapeutics. The authors declare no additional financial interests for the work presented here. The authors were solely responsible for the content and decision to publish.

Graphical Abstract

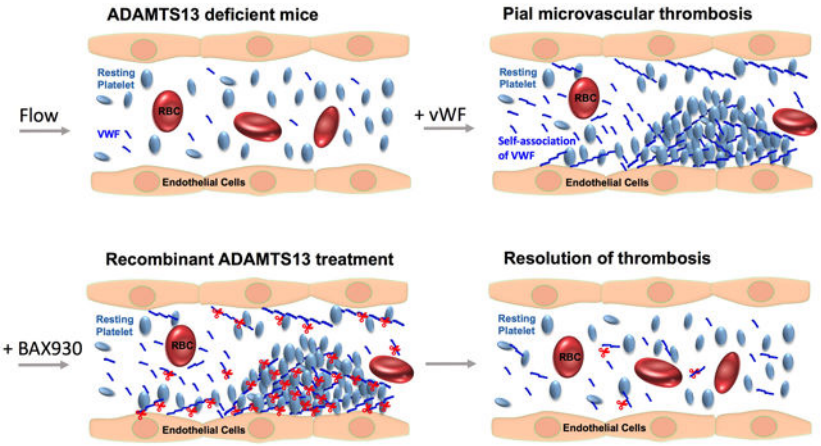

Keywords

TTP; cerebral microvascular thrombosis; VWF self-association; platelet adhesion thrombus resolution; rADAMTS13

Subject codes:

Vascular biology; Thrombosis

Introduction

Thrombotic thrombocytopenic purpura (TTP) is a rare but life-threatening disease characterized by profound thrombocytopenia, microangiopathic hemolytic anemia, and organ ischaemia.[1-3] Hereditary or acquired severe deficiency (<10% of the normal enzyme activity) of ADAMTS13 (a disintegrin and metalloproteinase with a thrombospondin type 1 motif, member 13), a von Willebrand factor (VWF) cleaving protease in plasma, is associated with the occurrence of TTP.[4, 5] In a healthy person, plasma ADAMTS13 cleaves endothelial cell-secreted ultra-large VWF (ULVWF) multimers into smaller, non-thrombogenic forms, thereby preventing spontaneous platelet adhesion and occlusive microvascular thrombosis. However, in the onset of microvascular thrombosis in TTP patients, the deficiency of ADAMTS13 results in an inability to cleave ULVWF and leads to adhesion of platelets on ULVWF via platelet surface glycoprotein Ibα (GPIbα) binding to the A1 domain of VWF.[6-8] The hallmark pathology of TTP is microvascular thrombosis in major organs such as the brain, liver, kidneys, heart, and pancreas, caused by unrestricted platelet adhesion to ULVWF multimers.[7, 9] Acute onset of TTP is a severe medical emergency, and plasma exchange therapy with or without immunosuppressive agents is the only first line therapy for TTP since it has been shown to be effective in reducing mortality from 90% to less than 20%.[3, 10]

Along with research advancements focused on understanding the pathogenesis of TTP, novel therapeutic strategies have been evaluated in both preclinical models [11-14] and current

clinical trials[15, 16] with promising results. These novel modalities include the development of recombinant ADAMTS13 (rADAMTS13)[16], nanobody targeting the A1 domain of VWF (Caplacizumab)[15], a GPIba receptor antagonist (Anfibatide)[17], and disulfide-bond reducing reagent N-acetylcysteine (NAC).[13, 18] All these strategies involve either 1) directly reducing the size of VWF multimers or 2) disruption of the platelet-VWF interaction to prevent the onset and development of microthrombosis. Microthrombosis is responsible for the severe platelet consumption, multiple organ failure, and microangiopathic hemolytic anemia associated with TTP. Since ADAMTS13 deficiency is the fundamental cause of TTP, rADAMTS13 is an emerging therapeutic currently under evaluation in preclinical models and clinical trials; these trials show promising results supporting the use of BAX930 for the treatment of TTP.[11, 12, 14, 19] In preclinical animal studies, both prophylactic and therapeutic administrations of BAX930 have been shown to effectively prevent the development of TTP-like symptoms, stabilize platelet counts, and prevent organ damage associated with microvascular thrombosis in mouse models of congenital TTP induced by recombinant VWF infusion. [11, 12, 14, 20] Furthermore, in a cerebral artery ischemia reperfusion model, ADAMTS13 regulation of VWF-platelet interactions has been shown to protect the brain from ischemia indicating rADAMTS13 may be a useful therapeutic agent for stroke.[21-24] Phase 1 studies of rADAMTS13 (BAX930) have recently reported favorable safety and pharmacokinetics[19], suggesting that recombinant ADAMTS13 would be an ideal therapeutic option for inherited TTP and might be a potential alternative therapy for acquired TTP when used in combination with plasma exchange therapy.

ADAMTS13 is an intriguing multidomain metalloprotease (Fig. 1) with VWF as its only known substrate. Regulation of ADAM-TS13 activity is unique as conformational changes in VWF are needed before proteolysis can occur [4–6]. Under nor-mal conditions, ultra-large (UL), hyperreactive VWF mul-timers are secreted from endothelial cells. Due to shear stress in flowing blood, they unfold and are processed by ADAMTS13 into normally sized, quiescent multimers (Fig. 2A). This process prevents spontaneous interaction between UL-VWF and the glycoprotein (GP) Ib/IX/V receptor on circulating platelets. In the absence of ADAM- TS13 activity, UL-VWF multimers can accumulate, leading to formation of disseminated thrombi that are rich in platelets and VWF. These microthrombi can block arterioles and capillariThe identification of ADAMTS13 mutations in hereditary TTP patients made ADAMTS13 knockout (KO) mice an attractive animal model to study for human congenital TTP.11,12 ADAMTS13 deficiency alone is insufficient to spontaneously develop TTP-like symptoms in mice, which limits the usage of this mouse model to study novel therapeutic approaches.[20, 25] Challenging of ADAMTS13 deficient (ADAMTS13$^{-/-}$) mice with intravenous infusion of high doses of recombinant human VWF containing ULVWF multimers circumvents this limitation; mice develop TTP-like symptoms similar to human patients, and this mouse model has been widely used as a congenital model for TTP to allow us to assess the efficacy of potential novel therapeutics.[14, 18, 26] Recombinant VWF (rVWF)- challenged ADAMTS13$^{-/-}$ mouse recapitulates many clinical manifestations and key elements in the pathology of TTP and is therefore useful for *in vivo* evaluation of potential therapy. However, pathological examinations of this model have consistently failed to detect microvascular thrombosis in brain vasculature, a primary pathological consequence of TTP that is known to lead to neurologic dysfunction in over 90% of patients.[27, 28]

Importantly, the rVWF-mediated onset of TTP in ADAMTS13$^{-/-}$ mice occurs in the absence of endothelial activation, and the mechanism by which circulating VWF in the plasma initiates thrombocytopenia and microthrombosis *in vivo* is not well studied. It is not clear whether the transfused exogenous rVWF containing ULVWF interacts with the endothelium on vessel wall and forms microvascular thrombosis when exposed to shear stress. Recently, the ability of VWF to self-associate has been highlighted in regulating the hemostatic activity of VWF.[29] VWF self-association is a complex process by which multimeric VWF homotypically associate or aggregates with additional VWF multimers upon exposure to shear stress. While the molecular mechanism of VWF self-association is not yet fully understood, the role of ADAMTS13 in preventing VWF self-association and in regulation of VWF size are well established.[30] Studies revealed that VWF self-association occurs *in vitro* under flow conditions, and this self-association of VWF into fibers supports platelet adhesion in microvessels, indicating that VWF self-association may play a role in pathological thrombosis.[31-33] However, it is not clear whether VWF self-association occurs *in vivo* or whether it is responsible for triggering the onset of microvascular thrombosis in the mouse model of TTP when VWF concentration increases acutely, especially when ADAMTS13 is absent. Additionally, TTP-like symptoms are poorly correlated to pathological findings of microthrombi. Thus, it is necessary to determine the onset and composition of microvascular thrombosis especially in the brain in mouse models of TTP and to further determine the efficacy of BAX930 on the resolution of cerebral microthrombosis.

MATERIALS AND METHODS

The data that support the findings of this study are available from the corresponding author upon reasonable request.

Animals

All experiments and animal care were approved by the University of Michigan Institutional Animal Care and Use Committee. ADAMTS13$^{-/-}$ mice (backcrossed>10 generations to C57BL/6J genetic background) were kindly provided by Dr. David Ginsburg (Department of Internal Medicine, University of Michigan, Ann Arbor, Michigan). Corresponding background matched wild-type (WT) C57BL/6J mice (stock: 000664) were purchased from the Jackson Laboratory (Bar Harbor, ME) and used as controls.

Materials

Recombinant human VWF (Shire, Vienna, Austria) and BAX930 were provided by Baxalta US Inc. (now part of Shire). rVWF (614 IU/per vial) was dissolved in 1mL of saline solution and the mice were challenged with 2000 U/kg rVWF (in 100uL of volume diluted with saline as needed based on the body weight of the mouse) via intravenous bolus injection. ADAMTS13 activity (3333.5U/mL), ADAMTS13 antigen level (2207.5 μg/mL) and total protein level (0.4948mg) of BAX930 were evaluated by Baxalta prior to shipment for use in the study. Mice were treated with 320 units/kg of BAX930 (diluted in 50uL of saline) via intravenous bolus injection. Same volume of saline solution was intravenously injected as a vehicle control for rVWF or BAX930 into control mice. For directly detecting of rVWF

binding to endothelial *in vivo*, rVWF was fluorescently labeled using an Alexa Fluor 488 dye (Invitrogen, USA) according to manufacturing instruction prior to injecting into mice.

rVWF-induced mouse model mimicking TTP

TTP in mice was provoked by intravenous injection of a high dose of rVWF in ADAMTS13$^{-/-}$ mice, a widely used well-established congenital mouse model of TTP as previously described.[11, 12, 14, 25] Briefly, ADAMTS13$^{-/-}$ mice (8–10 weeks old) were anesthetized using 2.5% isoflurane and 2000 U/kg rVWF was intravenously given via tail vein catheter to trigger a rapid development of TTP-like symptoms including severe thrombocytopenia, schistocytosis, a decrease in hematocrit, elevated serum lactate dehydrogenase levels, and organ damage, as has been well-characterized by several other groups.[11, 12, 14] Vehicle (saline solution) was injected into ADAMTS13$^{-/-}$ mice as a negative control. 2000 unit/kg rVWF was also injected into WT mice as a control for rVWF-induced thrombosis in ADAMTS13$^{-/-}$ mice mimicking TTP. All the procedures described above were performed in mice under intravital microscopy using real-time visualization of thrombosis and thrombolysis in the brain surface microvessels as described below.

Real-time intravital microscopy imaging

Cranial window imaging of brain microvascular thrombosis in mouse model of TTP—Brain microvascular thrombosis in ADAMTS13$^{-/-}$ mice induced by rVWF infusion was observed in real-time via cranial window imaging on brain surface vasculature via intravital microscopy as described.[34, 35] Briefly, ADAMTS13$^{-/-}$ mice were anesthetized with isoflurane and the mouse was positioned in a stereotactic head holder built on microscope stage adaptor equipped with gas mask and heating pad. Anesthesia was maintained with 2.5% isoflurane using a facial gas mask and mouse body temperature was maintained at 37 °C throughout the procedure using a heating pad controlled by a thermocontroller (Stoelting rodent warmer, Wood Dale, IL, USA). A tail vein catheter was established to administer antibodies and therapeutic reagents as needed. The surgical area was cleaned, and a 1 cm area of skin was excised on the dorsal surface of the skull over the right cortical hemisphere. A cranial window (3–4 mm in diameter) was surgically prepared using a high-speed drill under dissecting microscope (Olympus SZ61). A glass cover slip was placed on the cranial window and edges were sealed with Vetbond™ glue. Platelets in ADAMTS13$^{-/-}$ mice were fluorescently labeled by injecting DyLight 488- conjugated rat anti–mouse platelet GP1bβ antibody (0.1 μg/g; EMFRET Analytics) to visualize the platelets in blood flow in brain microvasculature as was carried out in previous studies.[36, 37] Then, the mouse in the stereotactic microscope stage adaptor was placed under an upright Zeiss Axio Examiner Z1 Advanced VIVO™ microscope (Intelligent Imaging Innovations) to visualize the pial microvessels using a X25 /0.8 numerical aperture oil immersion objective lens (Zeiss) or using a X10/0.3 air objective lens (Zeiss) through a high-speed sCMOS camera. All data were recorded and analyzed with SLIDEBOOK 6.0 (Intelligent Imaging Innovations) program. After 3 min prerecording, 2000 U/kg rVWF was intravenously given via tail vein catheter to induce TTP in mice.[14, 19] Brain microvasculature was continuously monitored in real-time for up to 90 min for the detection of thrombosis and cessation of blood flow. TTP was induced in a total of 15 ADAMTS13$^{-/-}$ mice by rVWF transfusion, and brain microvasculature was monitored and recorded using

real-time intravital microscopy. 5 ADAMTS13$^{-/-}$ mice (3 male and 2 female) were treated with vehicle control and 5 mice were intravenously given 320 units/kg of BAX930 prophylactic treatment 10 min prior to microscopy. The remaining 5 mice were given 320 units/kg of BAX930 intravenously when thrombosis reached approximately 70% of the vessel diameter occlusion, which happened 30 to 60 min after the bolus injection of 2000 U/kg rVWF via tail vein catheter. P-selectin expression on adhered platelets and platelets within microthrombi in mice were determined by injecting mice with Alexa Flour 647-rat anti-mouse CD62P antibody (BD Biosciences; 3 μg/per mouse) as reported previously.[38, 39] Fibrin formation within microthrombosis *in vivo* was detected by injecting mice with anti-fibrin labeled with Alexa Fluor 647, 0.3 μg/g) antibodies via jugular vein catheter prior to intravital microscopy imaging as described.[38, 39] To further confirm rVWF binding to endothelial *in vivo* in ADAMTS13 deficiency, Alexa Fluor 488-conjugated rVWF (2000 U/kg rVWF) were injected into ADAMTS13$^{-/-}$ mice following the injection of DyLight 649 conjugated rat anti–mouse platelet GP1bβ antibody for platelet labeling. Positive control images of platelet surface P-selectin expression and fibrin formation in thrombi *in vivo* were achieved by laser injury induced thrombosis in the pial microvessels of the brain under X40 1.0 air objective in experimental mice (3 mice).

Ionophore-provoked ULVWF-mediated microvascular thrombosis model— ADAMTS13$^{-/-}$ and WT recipient mice were anaesthetized and intravenously injected with fluorescently labeled platelets purified from the donor mice of the same genotype, and ionophore-provoked microvascular thrombosis in mesenteric venules was monitored in real-time under intravital microscopy as we characterized in our previously study.[13] Platelet preparation: Mice (6–8 weeks old) were anaesthetized by i.p. injection of ketamine/xylazine (100 mg/kg and 10 mg/kg body weight respectively), and whole blood was collected from the retro-orbital plexus using heparin-coated glass capillary tubes.[37] Blood was collected into a tube containing ACD (38 mM citric acid, 75 mM trisodium citrate, 100 mM dextrose). Platelet-rich plasma (PRP) was obtained by centrifugation of whole blood at 300 × g for 7 min. Gel-filtered platelets were then isolated from the PRP using a sepharose 2B column in PIPES buffer (PIPES 5 mM, NaCl 1.37 mM, KCl 4 mM, glucose 0.1%, pH 7.0). Platelet counts were confirmed using a Hemovet (HV950, Drew Scientific). Fluorescent labeling of gel-filtered platelets was achieved by incubating platelets with calcein-AM (1 μg/mL) for 15 min at room temperature. The efficacy of the fluorescent labeling of platelets was confirmed under fluorescent microscope prior to being used for in vivo imaging. Intravital microscopy imaging: 4-week-old mice were anesthetized and injected with fluorescently labeled platelets (1.25×10^6 platelets/g from mice of the same genotype). Mesenteric vessels were surgically prepared and monitored under an inverted fluorescent microscope (Zeiss Axio Observer Z1 Advanced Marianas™ Microscope) using a X20/04 numerical aperture air objective lens (Zeiss). An approximately 2.5mm section of the mesenteric venule (100 to 150 μM in diameter) was topically treated with 10 μL of 10 μM of calcium ionophore to induce Weibel-Palade body secretion of ULVWF from the endothelium, resulting in immediate adhesion of fluorescently labeled platelets and formation of platelet thrombi anchored to the vessel wall. For each mouse, the process of thrombosis and the resolution of thrombi were monitored and recorded for 20 min in addition to prerecording. BAX930 (320 units/kg) was administered via tail vein catheter 10 min prior to (prophylactic) or 2 min after

(therapeutic) the onset of thrombosis by calcium ionophore stimulation in mesenteric microvasculature in ADAMTS13$^{-/-}$ and WT mice (8 mice (4 male and 4 female) in each experimental group). The dynamics of platelet accumulation in selected vessel segments was quantitatively analyzed by 1) change in platelet fluorescent intensity over time 2) number of emboli (platelet thrombi larger than 20 μm in diameter) 3) thrombus resolution time: defined as the time required for platelet the fluorescence to return to near baseline following the topical application consistent with our previous study.[13]

Statistical analysis

Data are presented as mean ± standard error of the mean (SEM). Statistical significance was assessed by unpaired and paired Student t test and two-way analysis of variance (ANOVA) with Prism 6.0 software (GraphPad). All data were first subjected to Shapiro-Wilk normality test and F test to evaluate homogeneity of variances. For normally distributed data with similar variances among groups, unpaired Student t test with Welch correction was used for 2 group comparisons and 1-way ANOVA followed by Tukey test was used for more than 2 groups comparisons. Two-way ANOVA followed by Bonferroni test was applied for comparisons of grouped data under different conditions. Nonparametric Mann-Whitney test was used for data not normally distributed. $P< 0.05$ is considered significant.

Results

In the absence of ADAMTS13, soluble VWF self-associates on vessel walls to initiate platelet adhesion and pial microvascular thrombosis

To investigate whether rVWF transfusion in ADAMTS13$^{-/-}$ mice results in brain microvascular thrombus formation and to assess the initiation of microvascular thrombosis and platelet fibrin content of thrombi, a closed cranial window intravital microscopy approach was used as described previously.[34] The platelet-vascular wall interaction in the pial microvascular circulation in the brain was monitored in real-time in ADAMTS13$^{-/-}$ mice in response to rVWF challenge for up to 90 min. A dose of 2000 U/kg rVWF was chosen for the challenge in ADAMTS13$^{-/-}$ mice, as it was shown in previous studies to result in an acute increase of plasma VWF antigen (from 0.15 U/mL up to 55 U/mL) sufficient to provoke the TTP symptoms.[11] Fluorescent labeling of endogenous platelets was sufficient to observe the pial microvascular circulation in mice under intravital microscopy. As shown in Figure 1A (upper panel), as expected, platelet adhesion and aggregate formation was not detected in the brain microvasculature in ADAMTS13$^{-/-}$ mice treated with vehicle control prior to rVWF challenge. As shown in Figure 1A (lower pane), B and C, shortly after the bolus injection of rVWF into ADAMTS13$^{-/-}$ mice, circulating fluorescent platelets adhered to and formed visible platelet aggregates and microthromboses result in microvessel occlusion, which worsens over the time (movie 1 in the supplement). Capillary microvessels (approximately 10 μm in diameter) were more readily occluded than larger vessels and thrombi varied in time of appearance and location. Sporadic visible thrombi (>20 μm in diameter) were detected in both venules (move 2 in the supplement) and arterioles (move 3 in the supplement) as early as 5 min and as late as 90 min in different locations of pial microvessels. In real-time monitoring under higher magnification, we found that the infusion of rVWF led to the formation of long, loosely attached platelet strings that

were frequently washed downstream under the shear (Figure 2B (upper panel) and move 4 in the supplement). Some of the adhered platelet strings grew into platelet thrombi as observed in the microvasculature of ADAMTS13$^{-/-}$ mice. Additionally, observed platelet strings and sporadic thrombi varied in length (10 to 100 μm) and easily detached from vessel walls. Some adhered platelets grew into thrombi that momentarily attached to the vessel wall and occluded the vessels, resulting in the cessation of blood flow. The platelet micro-thrombosis worsened over the period of 90 minutes in rVWF challenged ADAMTS13$^{-/-}$ mice, and this is consistent with the reported kinetics of thrombocytopenia development in ADAMTS13$^{-/-}$ mice soon after the rVWF challenge. [11] VWF self-association on vessel walls and subsequent platelet adhesion seem to associate with the deficiency of ADAMTS13 as an intravenous bolus injection of the same dose of rVWF into WT mice did not result in thrombosis in the brain under the same experimental conditions (Figure 1E upper panel). Bolus injection of rVWF into WT mice only resulted in the immediate appearance of some floating platelet microaggregates in pial microvasculature but quickly cleared from pial microcirculation within a minute, as observed under high magnification (Figure 1E, lower panel). Finally, the binding of circulating soluble VWF to the endothelial surface of microvascular walls and subsequent VWF self-association was further confirmed by challenging ADAMTS13$^{-/-}$ mice with fluorescently labeled rVWF. As shown in Figure 2A and B, fluorescently labeled rVWF bound to endothelial surfaces and self-associated to form VWF fibers in ADAMTS13$^{-/-}$ mice. Platelets adhered onto endothelial bound VWF fibers, which resulted in the formation of platelet strings. We also observed VWF fibers along the vessel wall within microvascular thrombosis (shown by arrow).

Platelet activation and fibrin formation are not required for pial microvascular thrombosis in TTP *in vivo*

Deficiency of ADAMTS13 causes the VWF-mediated platelet aggregation and microvascular thrombosis in the arterioles and capillaries characteristic of TTP.[9] VWF is well-known for its interactions with platelet surface GPIba and glycoprotein IIb/IIIa (also known as integrin αIIbβ3), an indispensable receptor responsible for mediating platelet aggregation by binding to fibrinogen, VWF, and other ligands in plasma and platelets in the event of vascular injury.[37, 40] Unlike VWF-GPIbα binding, VWF binding to integrin αIIbβ3 requires platelet activation, as αIIbβ3 receptors exist in an inactive form on resting platelets. In order to determine whether VWF-GPIbα interaction in TTP causes platelet activation and αIIbβ3-mediated platelet aggregation *in vivo*, we determined platelet surface P-selectin expression and fibrin formation in pial microvascular circulation in ADAMTS13$^{-/-}$ mice challenged with rVWF under intravital microscopy. As was expected, circulating, fluorescently labeled platelets in ADAMTS13$^{-/-}$ mice were negative for P-selectin expression prior to rVWF challenge as observed via cranial window under intravital microscopy. As shown in Figure 1B, the vast majority of platelets adhered to platelet strings anchored to the vessel wall, formed occlusive microthrombi in arterioles, venules, and capillaries, and were negative for platelet surface P-selectin expression. Only a few individual platelets positive for P-selectin were observed and no notable increase in P-selectin expression was observed over time. Furthermore, fibrin was not detected in the observed microvascular thrombi in the brains of ADAMTS13$^{-/-}$ mice (Figure 1C), indicating that platelet activation and fibrin formation are not required for microvascular

thrombosis in the mouse model of TTP. Fibrin formation and P-selectin positive platelets were detectable with a laser injury induced thrombi in pial microvasculature in the brain of the same ADAMTS13$^{-/-}$ mice (Supplementary Figure 1). Thus, the development of microvascular thrombi in TTP mice was dramatically different from that of injury-induced thrombi.

Recombinant ADAMTS13 treatment effectively prevents and resolves pial microvascular thrombosis in a mouse model of TTP

The effectiveness of plasma transfusion for the treatment of TTP is derived from the substitution of ADAMTS13 and the simultaneous removal of circulating anti-ADAMTS13 autoantibodies present in patients with acquired TTP.[2, 3, 41] The effectiveness of rADAMTS13 has been proven *in vitro,* and rADAMTS13 has been shown to restore ADAMTS13 levels and ameliorate severe acquired TTP-like symptoms in a preclinical animal model of TTP induced by recombinant VWF transfusion and anti-ADAMTS13 antibodies.[12] Restoring the platelet count and reducing the severity of TTP-like symptoms has been the focus of many of these studies. In this study, we evaluated the prophylactic and therapeutic efficacy of BAX930 on the formation and resolution of cerebral microvascular thrombosis in our mouse model of TTP. To be consistent with previously published studies, a dose of 320 U/kg of rADAMTS13, which has been previously proven effective in prevention or therapeutic treatment of TTP-like symptoms in mouse models of TTP, was chosen for the current study. The therapeutic effects of rADAMTS13 (BAX930) were assessed in mice either immediately following the growth of detected microthrombi in pail venules to approximately 70% of vessel diameter, after 10 to 15 min of continuous growth (Figure 3A upper panel, movie 2 in the supplement), or after the complete vessel occlusion in pial arterioles as shown in Figure 3A (middle and lower panel, movie 3 in the supplement). Thrombus formation in pial venules was monitored from the time it began until it reached more than 70% occlusion, at which point a tail vein injection of BAX930 was immediately given. BAX930 treatment resulted in a notable resolution of growing thrombi, diminishing the thrombus size and preventing vessel occlusion during the observed time of 60 minutes post-treatment. Next, thrombus formation was captured in pial arteriole where full occlusion of the arteriole at the bifurcation was observed. The occlusive thrombus was visibly loose, forming small emboli but consistently growing and was continuously recorded for 20 minutes with vehicle treatment before BAX930 treatment. BAX930 treatment resolved the embolic thrombi and improved the blood flow and recanalization of arterioles, as the size of thrombi decreased over a 30 minute time period (Figure 3A lower panel and movie 3 in the supplement). Lastly, BAX930 treatment was initiated after complete vessel occlusion by thrombi formed in vehicle treated, rVWF challenged ADAMTS13. The occlusive thrombi were resolved by BAX930 treatment, and blood flow was partially restored following BAX930 treatment (Figure 3B). Taken together, BAX930 treatment resulted in a notable resolution of microaggregates, pre-formed thrombi, and growing thrombi and improved blood flow and vessel recanalization when percentage of vessel occlusion by thrombi was compared in different in size of vessels (Figure 3B left: <10μm and Figure 3B right: 10μm > in diameter) prior to and post BAX930 treatment (P<0.001 respectively). Consistent with these results, prophylactic treatment of BAX930 effectively

prevented the microvascular thrombosis in ADAMTS13$^{-/-}$ mice in respond to rVWF challenge (Figure 3C).

rADAMTS13 treatment attenuates platelet adhesion and accumulation on endothelial-bound ULVWF newly released from activated endothelial cells *in vivo*

Some limitations of this rVWF-mediated mouse model of TTP include the lack of endothelial activation, endothelial release of ULVWF and difficulty in the quantitative assessment of thrombus resolution. Thus, the efficacy of BAX930 on the formation and resolution of microthrombosis was further evaluated using an ionophore-provoked, ULVWF-mediated microvascular thrombosis model as was previously characterized in the mesenteric microvasculature in ADAMTS13$^{-/-}$ mice.[13] No platelet adhesion to the mesenteric vessel wall was detected under intravital microscopy recorded for 3 minutes prior to the application of ionophore in ADAMTS13$^{-/-}$ mice. As shown in Figure 4 (movie 5 and 6 in the supplement), topical application of calcium ionophore to the mesenteric vessel in ADAMTS13$^{-/-}$ mice resulted in secretion of ULVWF from activated endothelial cells in mesenteric venules, which lead to immediate accumulation of fluorescently labeled platelets. Accumulation of platelets often presented as single platelet strings apparently attached to endothelial-anchored ULVWF strands. Within minutes, thrombi containing multiple platelets formed and grew to 60% of the diameter of the treated vessels, but did not reach vessel occlusion, as they were loose and frequently embolized from the vessel wall. Interestingly, platelet adhesion and thrombosis in response to ionophore treatment was also observed in WT mice but it diminishes quickly as platelet adhesion was visibly less and thrombus size was much smaller in WT. Shown in Figure 4B, prophylactic BAX930 treatment but not vehicle treatment effectively prevented the ionophore -provoked platelet adhesion and thrombosis in ADAMTS13$^{-/-}$ mice. BAX930 treatment after 2 min of the onset of thrombosis was also immediately dampened the ongoing thrombosis in ADAMTS13$^{-/-}$ mice. Lastly, prophylactic or therapeutic BAX930 treatment was also inhibited the observed platelet adhesion and thrombosis in WT. (Figure 4C).

Quantitative analysis of platelet thrombotic response (Figure 5) in ADAMTS13$^{-/-}$ and WT mice is consistent with the visual observations *in vivo*. The analysis of the dynamics of platelet fluorescent intensity over the course of thrombotic response in ADAMTS13$^{-/-}$ mice showed that there was a robust increase in platelet fluorescent intensity with platelet accumulation, and each spike represents a platelet-containing thrombus as it formed in or flowed through the vessel being monitored. The fluorescence was not fully returned to near baseline due to repeated emboli formation (Figure 5A right). The increase of platelet fluorescent intensity in WT mice was less robust and spiky and the fluorescence was quickly returned to near baseline (5A left). Furthermore, thrombus formation and emboli formation were markedly enhanced in ADAMTS13$^{-/-}$ mice (Figure 5B), and the time required for thrombus resolution was significantly prolonged when compared to WT mice (Figure 5C). (The thrombus resolution time: WT control=6.5 ± 0.6 min and ADAMTS13$^{-/-}$ control =9.90 ± 0.99 min, $P<0.05$; the numbers of large thrombi (>20 μm in diameter) in WT control =8.9 ± 1.3; ADAMTS13$^{-/-}$ control mice=20.3 ± 1.9; $P<0.001$).

The prophylactic treatment with BAX930 in ADAMTS13$^{-/-}$ mice (Figure 4 and 5 and movie 7 in the supplement) resulted in a significant reduction in thrombus formation and emboli formation as compared to untreated controls (The thrombus resolution time=3.75 ± 0.82 min, P<0.001; the numbers of large thrombi =3.9 ± 1.1, P<0.001 when compared to untreated ADAMTS13$^{-/-}$ control mice respectively;). Therapeutic treatment with BAX930 in ADAMTS13$^{-/-}$ mice 2 minutes (Figure 4 and 5 and movie 8 in the supplement) after the onset of thrombosis effectively dampened the thrombotic response and significantly shortened the thrombus resolution time (The thrombus resolution =4.2 ± 0.8 min, P<0.001 when compared to untreated ADAMTS13$^{-/-}$ mice;) Similarly, the fact that prophylactic treatment with BAX930 in WT mice (Figure 4C and 5) was shown to be effective suggests that increasing ADAMTS13 levels in the plasma can accelerate resolution of ULVWF-platelet thrombi (The thrombus resolution time: BAX930 pretreated WT=3.9 ± 1.1 min, P<0.01; BAX930 post treated WT =6.0 ± 2.2 min; P>0.05 when compared to untreated WT mice respectively). Lastly, Platelets in mesenteric microvascular thrombi were mostly negative for platelet surface P-selectin expression, and no fibrin was detected, similar to our observation of cerebral microvascular thrombosis induced by rVWF in the current mouse model of cerebral TTP (Figure 6A and B).

Discussion

Neurological complications associated with microvascular thrombosis in the brain are the most common cause of death in TTP patients.[42] Clinical manifestations of TTP, especially in the brain, can range from headache or confusion to transient neurological deficit or coma as a result of ischemic stroke. Despite the dramatic response to plasma infusion or plasma exchange therapy in the acute onset of TTP, relapses remain common after the remission. Thus, understanding the underlying pathophysiology and determining therapeutic efficacy of emerging novel therapeutics on microvascular thrombosis in the brain in TTP are highly warranted.

In this study, we used the well-established rVWF-induced mouse model of TTP to determine the onset and composition of microvascular thrombi in the brain *in vivo* using a cranial window under intravital microscopy. We have demonstrated that acutely increasing the plasma concentration of VWF through rVWF transfusion results in the formation of microvascular thrombi in the brains of ADAMTS13$^{-/-}$ mice, and the kinetics of thrombosis and development of TTP-like symptoms are consistent with those reported for mouse models of TTP.[11, 14, 26] Further, we show that, unlike injury-induced thrombosis, platelet activation is not required for and fibrin formation is not involved in the onset of micro-thrombosis in mouse models of TTP triggered by rVWF. However, it is possible that platelet activation may be involved in later stages of TTP development in the presence of vascular injury in ischemic conditions. Thrombi in mouse models of TTP are structurally loose, unstable, and frequently embolize, which may explain the difficulty of finding thrombi, especially in the brain, in histopathologic studies in mice. While the mouse model of TTP resembles human TTP in many ways, the onset of microvascular thrombosis *in vivo* remains intriguing, as the portion of ULVWF multimers in rVWF is limited in addition to absence of endothelial activation in this model.[11, 43] Our study results from *in vivo* also demonstrated that, in the absence of ADAMTS13, soluble VWF, at high concentration, self-associates

with endothelial cells to provide a surface for platelet adhesion and initiates microvascular thrombosis under shear. The enhanced VWF self-association may likely be an important contributing factor for the increased platelet adhesion on VWF fibers and development of microvascular thrombosis in ADAMTS13$^{-/-}$ mice. The mechanism by which circulating plasma VWF is able to bind to resting endothelial surfaces and self-associate to provide an adhesive surface for platelet string formation under the shear stress is compelling. One potential explanation might be that, in the absence of ADAMTS13, a portion of ULVWF may be exposed and may persist on the endothelial surface, allowing soluble VWF to self-associate and provide a surface for platelet adhesion. Alternatively, endothelial cells have receptors that bind soluble VWF, and elevated concentrations of circulating VWF may allow for significant self-association. Further understanding the interaction between soluble VWF and endothelial cells and the dynamic self-association of VWF may have physiological significance in the onset and development of thrombosis, especially in relapse of TTP.

Importantly, our study results support that prophylactic and therapeutic treatment with BAX930 effectively reduces thrombosis and dissolves thrombi *in vivo*. To our knowledge, this is the first preclinical study focusing on brain microvascular thrombosis in TTP, and the first direct *in vivo* assessment of the efficacy of BAX930 treatment on thrombus formation and resolution. A potential limitation of the current study is that the study is limited to congenital mouse models of TTP, and future studies should assess whether BAX930 is effective in the presence of anti-ADAMTS13 antibodies such as those present in acquired TTP. While pial and cerebral microvessels appear to have many morphophysiolgical common properties, pial microvessels lack the ensheathment of astrocytes and the blood brain barrier properties that are characteristic of cerebral microvessels. Thus, our observation made in pial microvessels may not fully reflect cerebral microvascular thrombosis in TTP. Lastly, Study mice are not littermates. ADAMTS13$^{-/-}$ mice were bred in an animal facility at the University of Michigan and C57BL/6 mice were purchased from the Jackson Laboratory. Although ADAMTS13$^{-/-}$ mice were backcrossed to C57BL/6 for > 10 generations, it is possible that some background difference may still exist between these two mouse strains.

In summary, our study results in two complementary *in vivo* models which, when taken together, recapitulate the underlying pathology of cerebral microvascular thrombosis in TTP patients. We demonstrated that in the absence of ADAMTS13 activity, elevated levels of soluble VWF may lead to the onset of microvascular thrombosis via platelet accumulation onto VWF self-associated on vessel wall endothelium under shear conditions. Hence, the data presented here strongly indicate that rADAMTS13 administration may be an effective interventional therapy for microvascular thrombosis, the hallmark pathology in TTP.

Supplementary Material

Refer to Web version on PubMed Central for supplementary material.

Acknowledgments

R. Adili designed the study, performed the experiments, interpreted data and wrote the manuscript. M. Holinstat interpreted data, wrote the manuscript and supervised the research. All authors commented on manuscript drafts and approved the manuscript.

We thank Megan Hawley, Benjamin Tourdot and Zoe Zimmerman for carefully reviewing the manuscript and helpful suggestions. We thank Dr. Rodney M. Camire at Children's Hospital of Philadelphia for providing anti-mouse fibrin antibody for *in vivo* studies.

Sources of funding

This study was supported by a grant from Baxalta US Inc., part of Shire via the investigator-initiated grant H15–30723 (R. Adili and M. Holinstat). This study was also partially supported by the National Institute of Health Grants GM105671 (M. Holinstat) and HL114405 (M. Holinstat).

Nonstandard Abbreviations and Acronyms

TTP
thrombotic thrombocytopenic purpura

ADAMTS13
a disintegrin and metalloproteinase with a thrombospondin type 1 motif, member 13

VWF
von Willebrand factor

ULVWF
ultra-large von Willebrand factor

rVWF
recombinant von Willebrand factor

GPIbα
platelet surface receptor glycoprotein Ibα

rADAMTS13
recombinant ADAMTS13 protein

BAX930
recombinant ADAMTS13 from Shire (previously Baxalta)

glycoprotein IIb/IIIa
platelet surface receptor IIb/IIIa, also known as integrin αIIbβ3

References

1. Tsai HM. Current concepts in thrombotic thrombocytopenic purpura. Annu Rev Med. 2006;57:419–436 [PubMed: 16409158]
2. Sadler JE, Moake JL, Miyata T, George JN. Recent advances in thrombotic thrombocytopenic purpura. Hematology Am Soc Hematol Educ Program. 2004:407–423 [PubMed: 15561695]
3. Kremer Hovinga JA, Coppo P, Lammle B, Moake JL, Miyata T, Vanhoorelbeke K. Thrombotic thrombocytopenic purpura. Nat Rev Dis Primers. 2017;3:17020 [PubMed: 28382967]

4. Levy GG, Nichols WC, Lian EC, Foroud T, McClintick JN, McGee BM, Yang AY, Siemieniak DR, Stark KR, Gruppo R, Sarode R, Shurin SB, Chandrasekaran V, Stabler SP, Sabio H, Bouhassira EE, Upshaw JD Jr., Ginsburg D, Tsai HM. Mutations in a member of the adamts gene family cause thrombotic thrombocytopenic purpura. Nature. 2001;413:488–494 [PubMed: 11586351]
5. Zheng X, Chung D, Takayama TK, Majerus EM, Sadler JE, Fujikawa K. Structure of von willebrand factor-cleaving protease (adamts13), a metalloprotease involved in thrombotic thrombocytopenic purpura. J Biol Chem. 2001;276:41059–41063 [PubMed: 11557746]
6. Tsai HM. Thrombotic thrombocytopenic purpura: A thrombotic disorder caused by adamts13 deficiency. Hematol Oncol Clin North Am. 2007;21:609–632, v [PubMed: 17666281]
7. Sadler JE. Pathophysiology of thrombotic thrombocytopenic purpura. Blood. 2017;130:1181–1188 [PubMed: 28768626]
8. Zheng XL. Adamts13, ttp and beyond. Hereditary Genet. 2013;2:e104 [PubMed: 24790789]
9. Tsai HM. Mechanisms of microvascular thrombosis in thrombotic thrombocytopenic purpura. Kidney Int Suppl. 2009:S11–14 [PubMed: 19180123]
10. Joly BS, Coppo P, Veyradier A. Thrombotic thrombocytopenic purpura. Blood. 2017;129:2836–2846 [PubMed: 28416507]
11. Schiviz A, Wuersch K, Piskernik C, Dietrich B, Hoellriegl W, Rottensteiner H, Scheiflinger F, Schwarz HP, Muchitsch EM. A new mouse model mimicking thrombotic thrombocytopenic purpura: Correction of symptoms by recombinant human adamts13. Blood. 2012;119:6128–6135 [PubMed: 22529289]
12. Tersteeg C, Schiviz A, De Meyer SF, Plaimauer B, Scheiflinger F, Rottensteiner H, Vanhoorelbeke K. Potential for recombinant adamts13 as an effective therapy for acquired thrombotic thrombocytopenic purpura. Arterioscler Thromb Vasc Biol. 2015;35:2336–2342 [PubMed: 26338302]
13. Chen J, Reheman A, Gushiken FC, Nolasco L, Fu X, Moake JL, Ni H, Lopez JA. N-acetylcysteine reduces the size and activity of von willebrand factor in human plasma and mice. The Journal of clinical investigation. 2011;121:593–603 [PubMed: 21266777]
14. Kopic A, Benamara K, Piskernik C, Plaimauer B, Horling F, Hobarth G, Ruthsatz T, Dietrich B, Muchitsch EM, Scheiflinger F, Turecek M, Hollriegl W. Preclinical assessment of a new recombinant adamts-13 drug product (bax930) for the treatment of thrombotic thrombocytopenic purpura. J Thromb Haemost. 2016;14:1410–1419 [PubMed: 27371116]
15. Abdelghany MT, Baggett MV. Caplacizumab for acquired thrombotic thrombocytopenic purpura. N Engl J Med. 2016;374:2497
16. Scully M, Knobl P, Kentouche K, Rice L, Windyga J, Schneppenheim R, Hovinga JAK, Kajiwara M, Fujimura Y, Maggiore C, Doralt J, Hibbard C, Martell L, Ewenstein B. Recombinant adamts-13: First-in-human pharmacokinetics and safety in congenital thrombotic thrombocytopenic purpura. Blood. 2017;130:2055–2063 [PubMed: 28912376]
17. Lei X, Reheman A, Hou Y, Zhou H, Wang Y, Marshall AH, Liang C, Dai X, Li BX, Vanhoorelbeke K, Ni H. Anfibatide, a novel gpib complex antagonist, inhibits platelet adhesion and thrombus formation in vitro and in vivo in murine models of thrombosis. Thromb Haemost. 2014;111:279–289 [PubMed: 24172860]
18. Tersteeg C, Roodt J, Van Rensburg WJ, Dekimpe C, Vandeputte N, Pareyn I, Vandenbulcke A, Plaimauer B, Lamprecht S, Deckmyn H, Lopez JA, De Meyer SF, Vanhoorelbeke K. N-acetylcysteine in preclinical mouse and baboon models of thrombotic thrombocytopenic purpura. Blood. 2017;129:1030–1038 [PubMed: 28011677]
19. Marie Scully PK, Karim Kentouche, Lawrence Rice, Jerzy Windyga, Reinhard Schneppenheim, Kremer Hovinga Johanna A., Michiko Kajiwara, Yoshihiro Fujimura, Caterina Maggiore, Jennifer Doralt, Christopher Hibbard, Leah Martell and Bruce Ewenstein. A recombinant human adamts-13: First-in-human study evaluating pharmacokinetics, safety and tolerability in cttp patients. Blood online. 9 2017
20. Desch KC, Motto DG. Thrombotic thrombocytopenic purpura in humans and mice. Arterioscler Thromb Vasc Biol. 2007;27:1901–1908 [PubMed: 17525362]
21. Fujioka M, Hayakawa K, Mishima K, Kunizawa A, Irie K, Higuchi S, Nakano T, Muroi C, Fukushima H, Sugimoto M, Banno F, Kokame K, Miyata T, Fujiwara M, Okuchi K, Nishio K.

Adamts13 gene deletion aggravates ischemic brain damage: A possible neuroprotective role of adamts13 by ameliorating postischemic hypoperfusion. Blood. 2010;115:1650–1653 [PubMed: 19965676]

22. Nakano T, Irie K, Hayakawa K, Sano K, Nakamura Y, Tanaka M, Yamashita Y, Satho T, Fujioka M, Muroi C, Matsuo K, Ishikura H, Futagami K, Mishima K. Delayed treatment with adamts13 ameliorates cerebral ischemic injury without hemorrhagic complication. Brain Res. 2015;1624:330–335 [PubMed: 26254727]
23. Zhao BQ, Chauhan AK, Canault M, Patten IS, Yang JJ, Dockal M, Scheiflinger F, Wagner DD. Von willebrand factor-cleaving protease adamts13 reduces ischemic brain injury in experimental stroke. Blood. 2009;114:3329–3334 [PubMed: 19687510]
24. Khan MM, Motto DG, Lentz SR, Chauhan AK. Adamts13 reduces vwf-mediated acute inflammation following focal cerebral ischemia in mice. J Thromb Haemost. 2012;10:1665–1671 [PubMed: 22712744]
25. Vanhoorelbeke K, De Meyer SF. Animal models for thrombotic thrombocytopenic purpura. J Thromb Haemost. 2013;11 Suppl 1:2–10
26. Muchitsch EM, Dietrich B, Rottensteiner H, Auer W, Nehrbass D, Gritsch H, Ehrlich HJ, Turecek PL, Schwarz HP. Preclinical testing of human recombinant von willebrand factor: Adamts13 cleavage capacity in animals as criterion for species suitability. Semin Thromb Hemost. 2010;36:522–528 [PubMed: 20632249]
27. Meloni G, Proia A, Antonini G, De Lena C, Guerrisi V, Capria S, Trisolini SM, Ferrazza G, Sideri G, Mandelli F. Thrombotic thrombocytopenic purpura: Prospective neurologic, neuroimaging and neurophysiologic evaluation. Haematologica. 2001;86:1194–1199 [PubMed: 11694406]
28. Gruber O, Wittig L, Wiggins CJ, von Cramon DY. Thrombotic thrombocytopenic purpura: Mri demonstration of persistent small cerebral infarcts after clinical recovery. Neuroradiology. 2000;42:616–618 [PubMed: 10997569]
29. Lopez JA, Chung DW. Vwf self-association: More bands for the buck. Blood. 2010;116:3693–3694 [PubMed: 21071615]
30. Chen J, Chung DW. Inflammation, von willebrand factor, and adamts13. Blood. 2018;132:141–147 [PubMed: 29866815]
31. Savage B, Sixma JJ, Ruggeri ZM. Functional self-association of von willebrand factor during platelet adhesion under flow. Proc Natl Acad Sci U S A. 2002;99:425–430 [PubMed: 11756664]
32. Yuan H, Deng N, Zhang S, Cao Y, Wang Q, Liu X, Zhang Q. The unfolded von willebrand factor response in bloodstream: The self-association perspective. J Hematol Oncol. 2012;5:65 [PubMed: 23067373]
33. Dayananda KM, Singh I, Mondal N, Neelamegham S. Von willebrand factor self-association on platelet gpibalpha under hydrodynamic shear: Effect on shear-induced platelet activation. Blood. 2010;116:3990–3998 [PubMed: 20696943]
34. Zuluaga-Ramirez V, Rom S, Persidsky Y. Craniula: A cranial window technique for prolonged imaging of brain surface vasculature with simultaneous adjacent intracerebral injection. Fluids and barriers of the CNS. 2015;12:24 [PubMed: 26507826]
35. Goldey GJ, Roumis DK, Glickfeld LL, Kerlin AM, Reid RC, Bonin V, Schafer DP, Andermann ML. Removable cranial windows for long-term imaging in awake mice. Nat Protoc. 2014;9:2515–2538 [PubMed: 25275789]
36. Adili R, Tourdot BE, Mast K, Yeung J, Freedman JC, Green A, Luci DK, Jadhav A, Simeonov A, Maloney DJ, Holman TR, Holinstat M. First selective 12-lox inhibitor, ml355, impairs thrombus formation and vessel occlusion in vivo with minimal effects on hemostasis. Arterioscler Thromb Vasc Biol. 2017;37:1828–1839 [PubMed: 28775075]
37. Reheman A, Yang H, Zhu G, Jin W, He F, Spring CM, Bai X, Gross PL, Freedman J, Ni H. Plasma fibronectin depletion enhances platelet aggregation and thrombus formation in mice lacking fibrinogen and von willebrand factor. Blood. 2009;113:1809–1817 [PubMed: 19036705]
38. Adili R, Tourdot BE, Mast K, Yeung J, Freedman JC, Green A, Luci DK, Jadhav A, Simeonov A, Maloney DJ, Holman TR, Holinstat M. First selective 12-lox inhibitor, ml355, impairs thrombus formation and vessel occlusion in vivo with minimal effects on hemostasis. Arterioscler Thromb Vasc Biol. 2017

39. Adili R, Voigt EM, Bormann JL, Foss KN, Hurley LJ, Meyer ES, Veldman AJ, Mast KA, West JL, Whiteheart SW, Holinstat M, Larson MK. In vivo modeling of docosahexaenoic acid and eicosapentaenoic acid-mediated inhibition of both platelet function and accumulation in arterial thrombi. Platelets. 2017:1–9

40. Ni H, Denis CV, Subbarao S, Degen JL, Sato TN, Hynes RO, Wagner DD. Persistence of platelet thrombus formation in arterioles of mice lacking both von willebrand factor and fibrinogen. The Journal of clinical investigation. 2000;106:385–392 [PubMed: 10930441]

41. Tsai HM. Von willebrand factor, adamts13, and thrombotic thrombocytopenic purpura. Journal of molecular medicine. 2002;80:639–647 [PubMed: 12395148]

42. Tsai HM. Platelet activation and the formation of the platelet plug: Deficiency of adamts13 causes thrombotic thrombocytopenic purpura. Arteriosclerosis, thrombosis, and vascular biology. 2003;23:388–396

43. Turecek PL, Schrenk G, Rottensteiner H, Varadi K, Bevers E, Lenting P, Ilk N, Sleytr UB, Ehrlich HJ, Schwarz HP. Structure and function of a recombinant von willebrand factor drug candidate. Semin Thromb Hemost. 2010;36:510–521 [PubMed: 20635317]

Highlights:

- Microvascular thrombosis in the brain is the hallmark pathology of TTP.
- At high levels, VWF self-association initiates cerebral microvascular thrombosis in the absence of ADAMTS13.
- Platelet activation and fibrin formation are not required for cerebral microvascular thrombosis *in vivo*
- Administration of rADAMTS13 effectively resolves microvascular thrombosis in the brain.

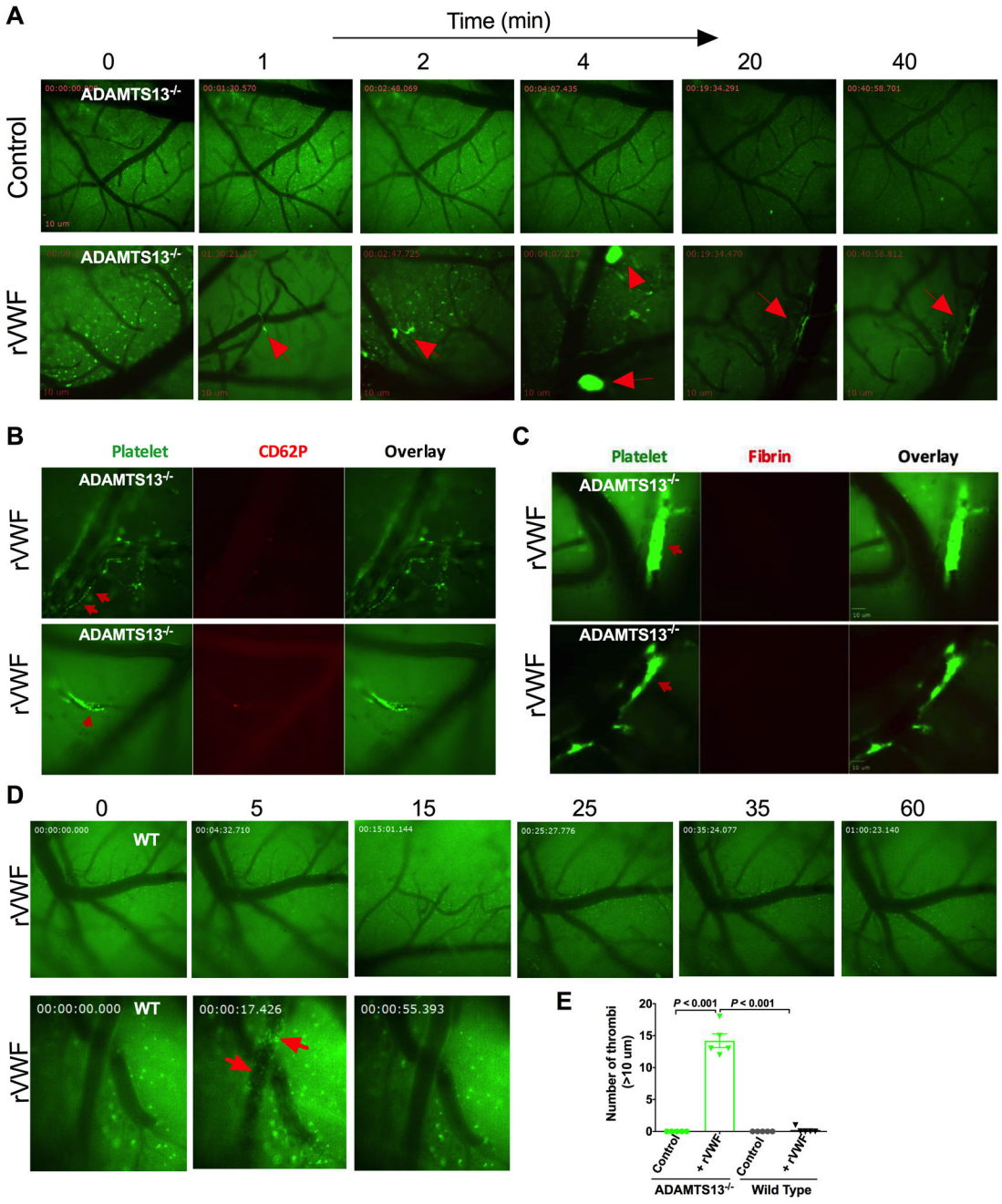

Figure 1. Initiation and development of VWF-triggered microvascular thrombosis in the brain in mouse model TTP.

A: Formation of microvascular thrombosis induced by rVWF: ADAMTS13$^{-/-}$ mice were intravenously injected with vehicle control or rVWF (2000 U/kg) and pial microvasculature in the brains was monitored in real-time via a cranial window under intravital microscopy for 60 minutes. Platelets were fluorescently labelled as green and pial microvessels in the brain are shown in dark. Transfusion of high dose of VWF in ADAMTS13$^{-/-}$ resulted in platelet adhesion, initiated thrombus formation and caused vessel occlusion in pial microvasculature in the brain under the shear condition. Thrombi formation (shown in bright

green) in pail microvasculature in ADAMTS13$^{-/-}$ mice following the rVWF challenge are indicated by arrows. Still images were taken at the indicated times shown above after the infusion of rVWF in ADAMTS13$^{-/-}$ mice. **B:** VWF self-association on vascular wall endothelium surface and platelet P-selectin expression: Upper panel: Shortly after rVWF infusion into ADAMTS13$^{-/-}$ mice, soluble VWF in plasma bound to vascular wall endothelium surface and self-associated under shear to trigger platelet adhesion and thrombosis. Fluorescently-labeled platelets adhered onto the endothelial bound VWF fibers and formed long platelet strings (upper panel, indicated by arrow) that led to microvascular thrombosis (lower panel, indicated by arrow) under shear in pial microvasculature in the brains of ADAMTS13$^{-/-}$ mice detected with higher objective (25X) under multi-channel intravital microscopy. The majority of adhered platelets and platelets within the growing thrombi were negative for P-selectin expression on their surface except for a few single platelets shown positive for P-selectin detected by anti-mouse CD62P antibody *in vivo*. **C**: Detection of fibrin formation in microthrombi in the brain: unlike injury-induced thrombosis, fibrin formation was not detected in rVWF-triggered microvascular thrombosis in pial microvessels in the brain. Fibrin formation within platelet thrombi in pial microvasculature in three different ADAMTS13$^{-/-}$ mice was examined *in vivo* using fluorescently labeled anti-mouse fibrin antibody, and no fibrin formation was detected within thrombi (n= 5) in the period of 60 min recording. **D:** Platelet adhesion and thrombosis was not detected in the brain microvessels in wild type (WT) mice after rVWF (2000 U/kg) challenge (upper panel). Bolus injection of rVWF resulted in an immediate presence of circulating platelet micro aggregates in pial microvasculature (lower panel) detected with higher objective (25X) but quickly cleared from blood circulation in less than a minute. rVWF challenge in WT mice did not result in VWF fibrillar and platelet string formation on endothelial surface on vessel wall *in vivo*. E: Quantitative analysis of pial microvascular thrombi larger than 10 μm in diameter following the vehicle control or rVWF challenge in ADAMTS13$^{-/-}$ and WT mice.

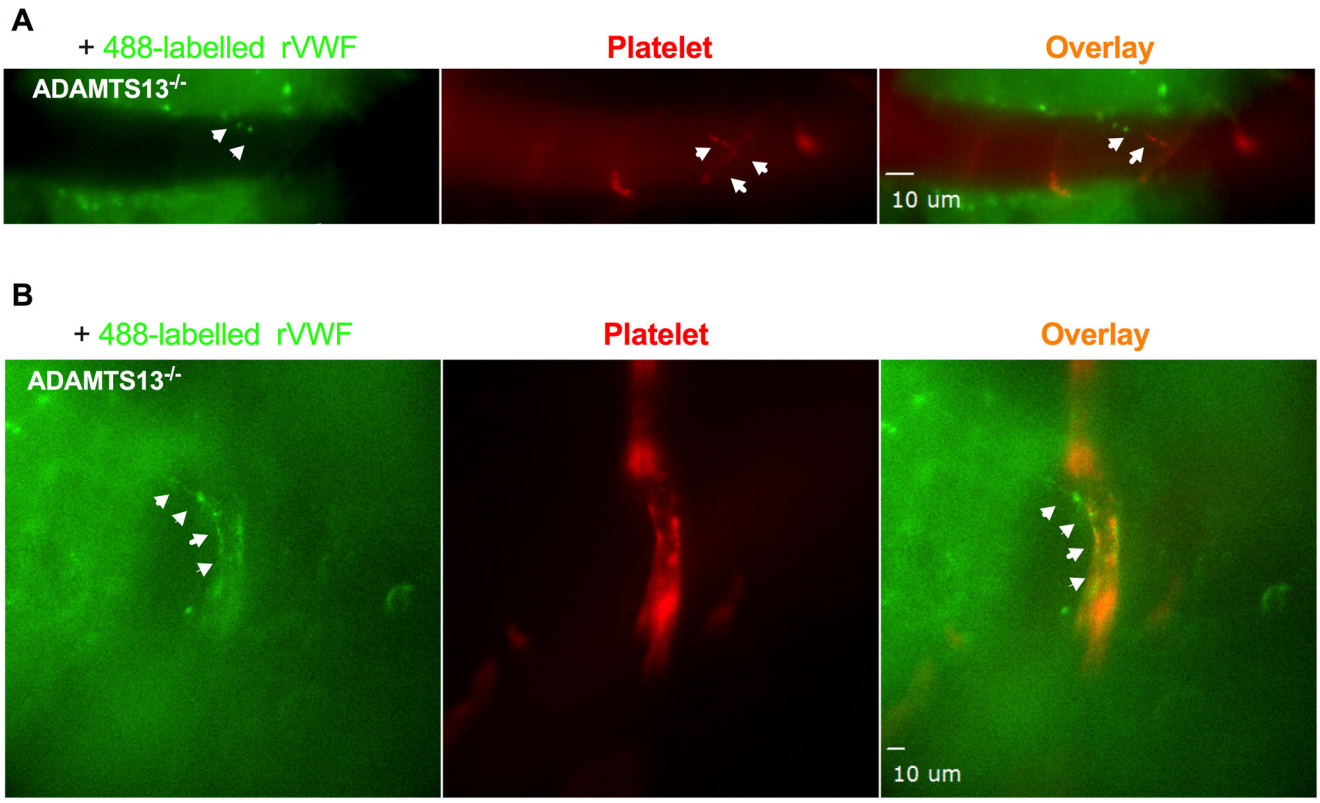

Figure 2. Exogenous recombinant VWF bind to the endothelial surface of pial microvascular wall and VWF self-associate to trigger platelet adhesion and thrombosis.

Alexa Fluor 488-conjugated rVWF (Green) were intravenously injected to ADAMTS13$^{-/-}$ mice and monitored in real-time by intravital microscopy for endothelial interaction, platelet adhesion and thrombosis in pial microvascular circulation. Platelets in ADAMTS13$^{-/-}$ mice were fluorescently labeled using a DyLight 649-conjugated GP1bβ antibody (Red). **A:** Fluorescently labeled rVWF bound to vascular wall endothelium surface, self-associated to form ULVWF fibers (left panel, indicated by arrows). Adhered platelets on endothelial-bound ULVWF are shown in red (middle panel, indicated by arrows). Adhered platelets on ULVWF are shown as platelet string in overlaid image. (right panel indicated by arrows). **B:** VWF fibers along the vessel wall within microvascular thrombosis detected with higher objective (25X) under multi-channel intravital microscopy.

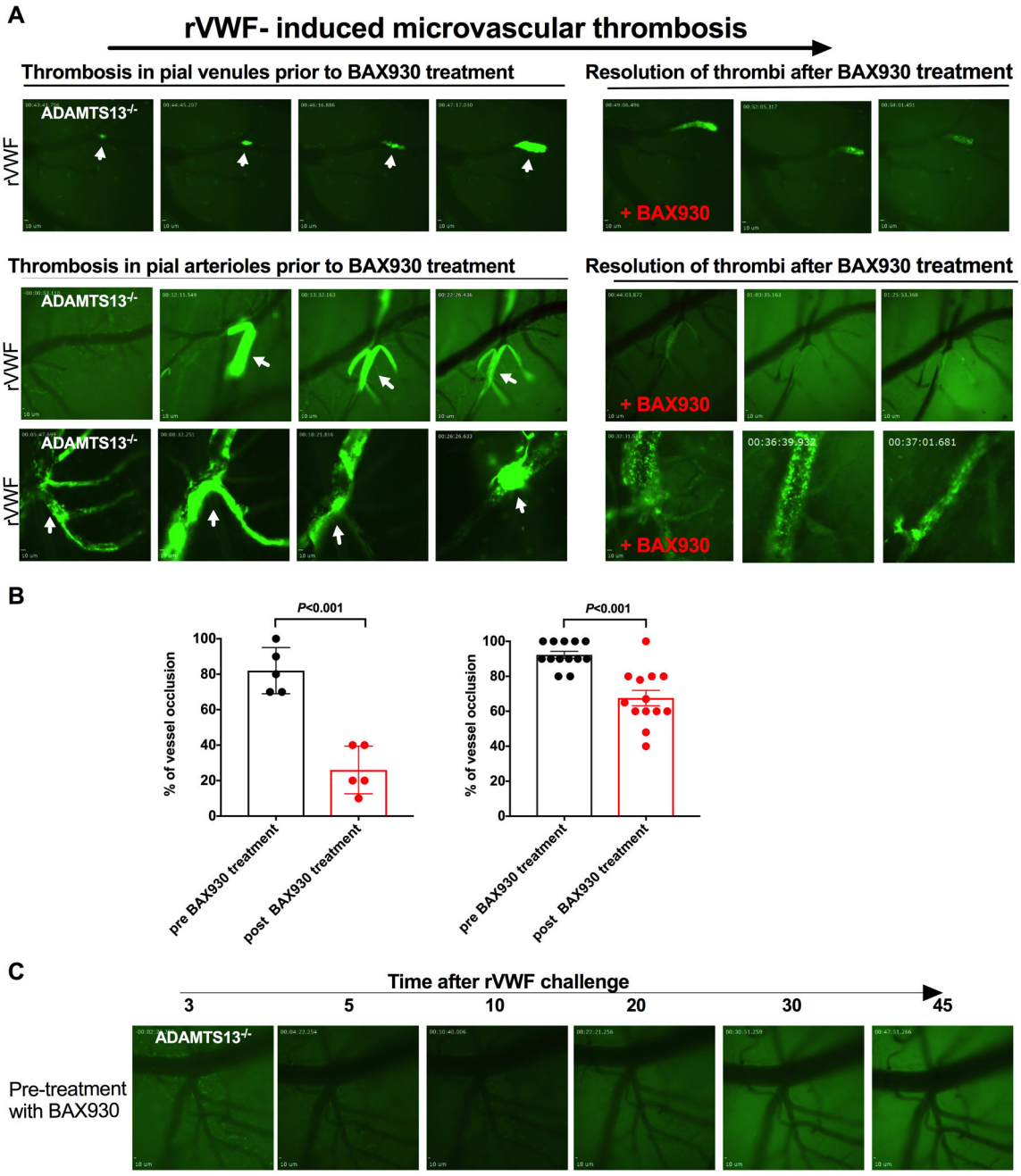

Figure 3. Recombinant ADAMTS13 treatment effectively resolves pre-existing and growing microvascular thrombi in the brain in a mouse model of TTP.

A: Representative images of microvascular thrombosis formed in the brain of 3 different ADAMTS13$^{-/-}$ mice following the transfusion of rVWF and the effect of BAX930 treatment. Pial microvasculature in the brain in ADAMTS13$^{-/-}$ mice is shown in dark and formed thrombi are shown in bright green. Thrombus formation in pial microvessels prior to BAX930 treatment are shown on the left and effect of rADAMTS13 treatment on thrombosis are shown on the right. Thrombi were observed for up to 60 minutes under the cranial window intravital microscopy. Upper panel: Thrombus formation in the pial venule

was monitored from onset until it reached more than 70% occlusion, at which point an immediate tail vein injection of BAX930 was given. Thrombus growth was immediately attenuated, and the thrombi resolved. Lower panel arteriole 1: Thrombus formation was captured occluding the pial arteriole at the bifurcation. The thrombus was visibly loose, forming small emboli but consistently growing for the next 20 min before BAX930 treatment. BAX930 treatment resolved the embolic thrombi, improved the blood flow, and decreased the size of the thrombi over time. Arteriole 2: Vessel occlusion by thrombus in pial arteriole was captured in ADAMTS13$^{-/-}$ mice pretreated with the vehicle control. BAX930 treatment was initiated after vessel occlusion to observe the resolution of the thrombus. The thrombus was resolved, and blood flow was partially restored by BAX930 treatment. Pial microvasculature in the brain in ADAMTS13$^{-/-}$ mice is shown in dark and time elapsed since the VWF infusion is indicated. **B:** Quantitative analysis of the effect of BAX930 treatment on vessel occlusion. Left: comparison of percentage of vessel (<10 μm in diameter) occlusion by thrombi pre and post BAX930 treatment. (P< 0.001 n= 5;) Right: comparison of percentage of vessel (>10 μm in diameter) occlusion by thrombi pre and post BAX930 treatment. (P< 0.001 n= 13;) **C:** Prophylactic treatment with BAX930 protected ADAMTS13$^{-/-}$ mice from microvascular thrombosis in the brain following the VWF challenge. Times after rVWF challenge in ADAMTS13$^{-/-}$ mice is indicated above. 5 mice in each group were studied.

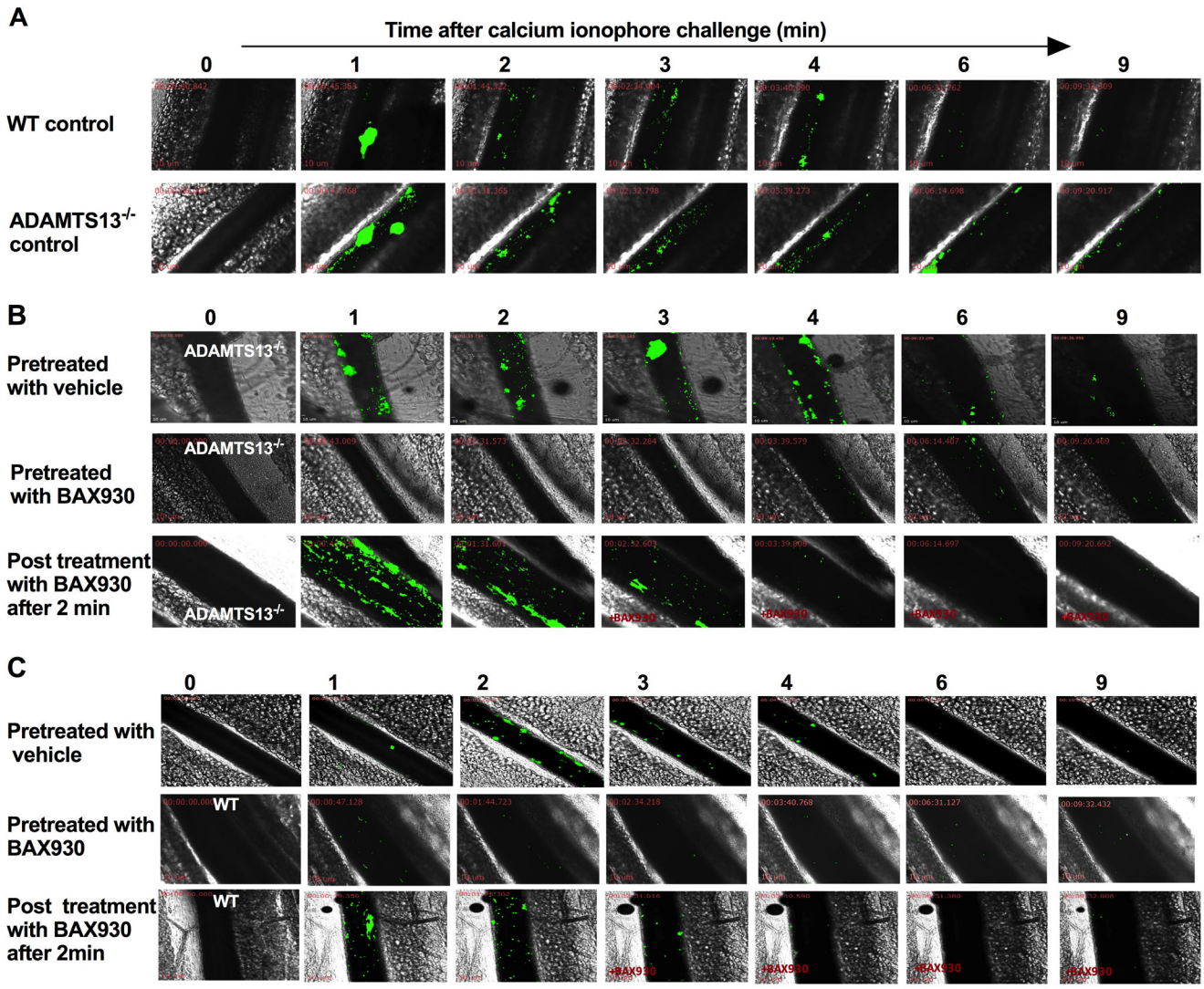

Figure 4. Recombinant ADAMTS13 (a disintegrin and metalloproteinase with a thrombospondin type 1 motif, member 13) treatment attenuates platelet accumulation on newly released endothelial-bound ULVWF (ultra-large von Willebrand factor) in vivo.

Mesenteric venules of ADAMTS13$^{-/-}$ mice were topically treated with calcium ionophore to release ULVWF from the endothelium of vessel wall and platelet adhesion and accumulation on endothelial-bound ULVWF was monitored in real-time under intravital microscopy. Florescent platelets are shown in green and sequential images taken at the indicated times after the application of calcium ionophore are aligned. **A:** Representative sequential images of VWF mediated platelet adhesion and thrombosis in WT (upper panel) and ADAMTS13$^{-/-}$ mice (lower panel). Ionophore-provoked thrombosis was enhanced and prolonged in ADAMTS13 deficiency. **B:** Representative sequential images of ionophore-provoked thrombosis in ADAMTS13$^{-/-}$ mice treated with vehicle control or BAX930 treatment. Upper panel: ADAMTS13$^{-/-}$ mice pretreated with vehicle control; Middle panel: ADAMTS13$^{-/-}$ mice pretreated with BAX930 10 min prior to calcium ionophore application; Lower panel: ADAMTS13$^{-/-}$ mice treated with BAX930 2 min after the onset of thrombosis following the calcium ionophore application. Prophylactic and therapeutic

BAX930 treatment in ADAMTS13$^{-/-}$ mice effectively prevented and immediately resolved the growing thrombi in mesenteric venules. **C:** Representative sequential images of ionophore-provoked thrombosis in WT mice treated with vehicle control or BAX930 treatment. Upper panel: WT mice pretreated with vehicle control; Middle panel: WT mice pretreated with BAX930 10 min prior to calcium ionophore application; Lower panel: WT mice treated with BAX930 2 min after the onset of thrombosis following the calcium ionophore application. Prophylactic BAX930 treatment in WT effectively inhibited thrombosis in response to calcium ionophore. Therapeutic BAX930 treatment in WT mice immediately resolved the growing thrombi in mesenteric venules. 8 mice were examined in each group.

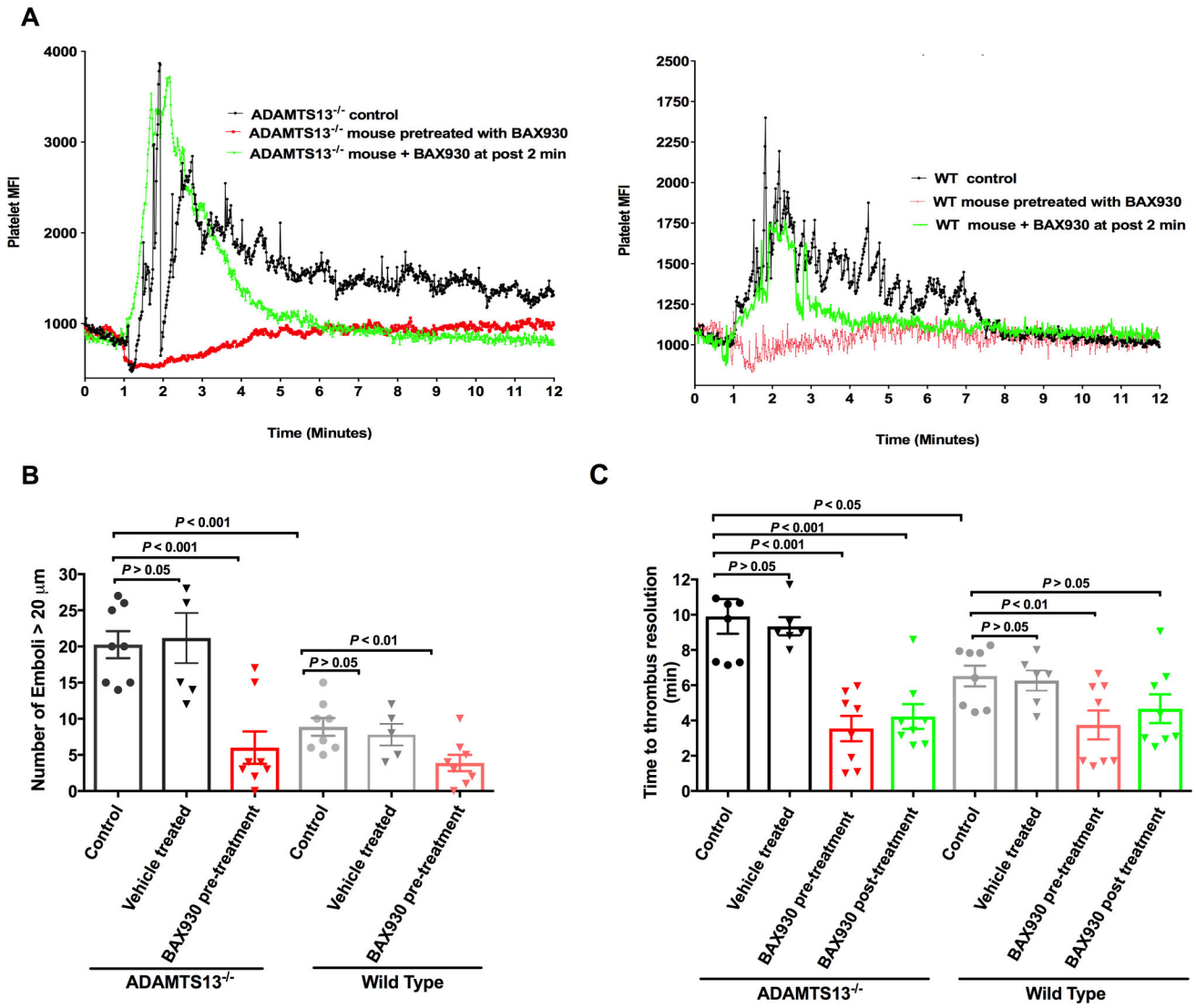

Figure 5. Quantitative analysis of platelet accumulation and emboli formation in ionophore-provoked ULVWF-mediated mesenteric microvascular thrombosis model:

A: Representative traces of dynamics of platelet accumulation quantified by platelet fluorescent intensity over time in vehicle treated control ADAMTS13$^{-/-}$ mice (Left) and WT mice (Right) are shown in black color. Topical application of calcium ionophore on the mesenteric venules resulted in a sharp increase in platelet mean fluorescence intensity (MFI) as a result of platelet thrombus formation followed by drop in platelet MFI by many spikes representing embolization of thrombi in the vessel segment being monitored until ultimately returning to baseline level. The peak platelet MFI in ADAMTS13$^{-/-}$ mice was significantly higher than that of WT mice (P<0.05) due to enhanced thrombotic response in ADAMTS13 deficiency. Fluctuation in platelet MFI was more notable in ADAMTS13$^{-/-}$ mice (as compared to WT mice) due to larger size and prolonged emboli formation. Prophylactic BAX930 treatment in both ADAMTS13$^{-/-}$ mice and WT mice (shown in red) effectively prevented platelet adhesion and formation of platelet thrombi (ADAMTS13$^{-/-}$ P<0.001, WT P<0.01). Therapeutic administration of BAX930 in both ADAMTS13$^{-/-}$ mice and WT

(shown in green) at 2 min after the onset of thrombosis induced by ionophore application acutely attenuated thrombus formation and accelerated thrombus resolution. **B:** Quantification of emboli formation. Number of large emboli (>20 μm in diameter) formed in mesenteric venules of ADAMTS13$^{-/-}$ (column 1 to 3) or WT mice (column 4 to 6) that untreated or pretreated with vehicle control (black: ADAMTS13$^{-/-}$, grey: WT) or pretreated with BAX930 (shown in red) in response to calcium ionophore treatment. Significantly more emboli were formed in ADAMTS13$^{-/-}$ mice when compared to WT. Prophylactic BAX930 treatment effectively inhibited thrombus formation in both ADAMTS13$^{-/-}$ and WT mice. **C**. Thrombus resolution time. Time required for the platelet the fluorescence returning to near baseline following the topical application in ADAMTS13$^{-/-}$ (column 1 to 4) or WT mice (column 5 to 8) that untreated or pretreated with vehicle control (black: ADAMTS13$^{-/-}$, grey: WT) or pretreated with BAX930 (shown in red) or BAX930 post treatment (green). Time for thrombus resolution was significantly longer in ADAMTS13$^{-/-}$ mice when compared to WT. Thrombus resolution time was significantly shorter in both pre and post BAX930 treated ADAMTS13$^{-/-}$ mice. Thrombus resolution time in WT was significantly shortened by prophylactic BAX930 treatment.

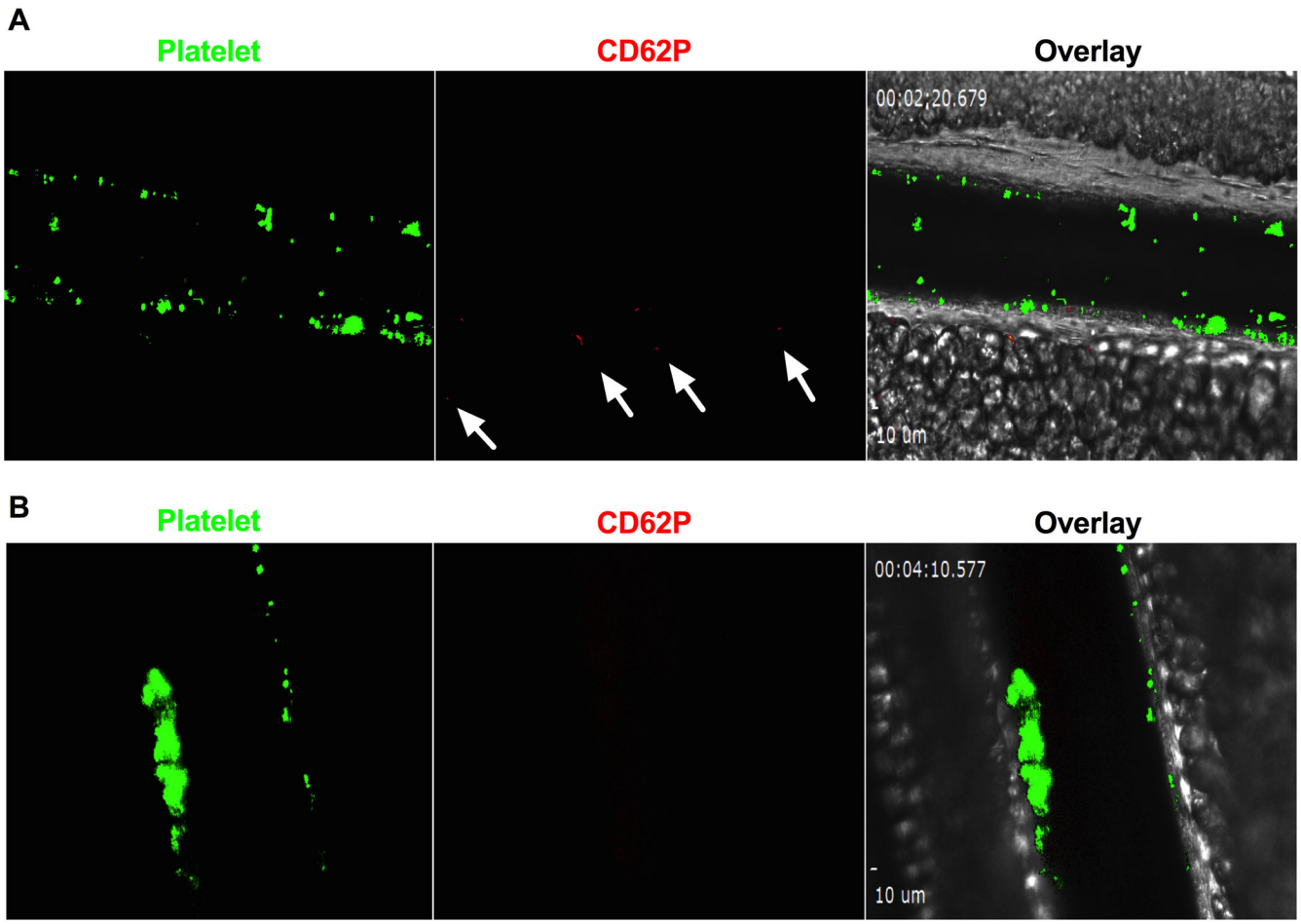

Figure 6: Platelet surface P-selectin expression and fibrin formation in ionophore-provoked microvascular thrombosis model.

A: Platelets in ADAMTS13$^{-/-}$ were fluorescently labelled as green and platelet surface P-selectin was detected by anti-P-selectin antibody (red) *in vivo*. P-selectin expression was not detected on the majority of platelets within thrombi except for the few platelets shown to be positive for P-selectin (indicated by arrows). **B:** Fibrin formation in thrombi: Fibrin formation was not detected in ionophore-provoked ULVWF-mediated microvascular thrombosis in mesenteric microvascular thrombosis in ADAMTS13$^{-/-}$ mice (n=3). Positive images of P-selectin and fibrin formation were confirmed by laser injury induced thrombosis in the same mice (shown in the supplementary).